



Research on Intelligent Joint Dispatch Control of Large-scale Water Conservancy Hub Gate Dam Groups Based on Multi-agent Collaboration Technology

Nan Zhu^{1,*}

¹ College of Engineering, City University of Hong Kong, Hong Kong, 999077, China

SUMMARY: *Due to the fast development of deep reinforcement learning technology in recent years, the excellent decision-making ability provided by it has shown great success in various optimization problems. In this context, an intelligent joint optimization and control method based on the multi-agent technology is proposed for large-scale water conservancy hub gate-dam complexes in this paper. First, studies about intelligent gate control for dam gate complexes using reinforcement learning technology are reviewed. Using reinforcement learning algorithm, a multi-agent reinforcement learning model was built using real-time monitoring information and optimal gate control simulation information. Further using this model, this paper also proposed a decomposed multi-agent method to address multi-objective flood control scheduling problems for dam complexes. By decomposing the problem into several sub-problems, different reinforcement learning agents will be used to generate an optimal solution set. This approach was validated by using simulation including the process of actual flood changes when scheduling dams, calculating reservoir water storage amounts and comparing it with measurements. Through the coordinated regulation, the total storage capacity can increase by 7.19 million m³, 9.88 million m³, and 11.36 million m³ at Liuqiao, Gongjia, and Baoji sluice gates respectively. As the amount of floods increases, the storage capacity also grows proportionally, almost twice as much as the real-world storage amount.*

KEYWORDS: *Multi-agent; Reinforcement learning; Dam cluster; Joint operation*

1 Introduction

The large-scale construction of water conservancy projects can bring about various socio-economic advantages through the exploitation of water resources for flood prevention, water provision, irrigation, and electricity production. Therefore, the exploitation of such projects offers considerable socio-economic assistance [1, 2]. Scientific scheduling is necessary to ensure that water resources can be effectively and reasonably exploited when water conservancy hubs operate normally [3]. A hydraulic hub project consists of the structures such as dam, gate, sluice, and power station. Among all of those facilities, the dam plays a vital role in regulating the water level and controlling the water discharge, while the gate and sluice take charge of controlling the water level and preventing flood or drainage. Electricity production depends on hydropower [4, 5]. Integrated scheduling of water conservancy hubs is very difficult and important, since integrated scheduling contributes to the optimization of exploitation and comprehensive utilization of water resources [6, 7].

Traditional gate and dam controlling techniques included water resource dispatchers

*nanzhu6-c@my.cityu.edu.hk

<https://doi.org/10.65102/is2026147>

sending schedule instructions to power station operators by means of fax or telephone communication. Such an approach decreased the number of gate operations and consequently shortened the lifetime of valves; in addition, the use of information about the current state of dam structures and weather forecasting faced problems of delay and inadequate coordination [8, 9]. The development of large-scale water conservancy hub dispatch management together with the development of intelligent dispatch technologies makes conventional gate and dam controlling schemes inappropriate any longer. The introduction of intelligent technologies will help implement intelligent dispatching and controlling for water conservancy project hub facilities in a variety of situations [10-13]. To address the problem of using intelligent technologies to substantially decrease the labor intensity of the operators while guaranteeing reliability and safety, thereby liberating the productive forces, research is needed regarding how to conduct coordinated cooperation between large-scale water conservancy hub gate and dams for remote scheduling and control.

Model-based regulation control system for cascade hydropower plant gates has been used by Mou et al. [14], where the control was done through offline calculations and online searches under the condition of high intensity peak shaving and frequency regulation. Intelligent cranes have been used to perform gate operations at run-of-river hydropower plants by Yang et al. [15], which makes it possible to do one-button multi-objective gate switching. In this case, the performance of the task is improved in terms of efficiency without compromising on safety. Dam gate control system has been designed by Hamidun and Ibrahim [16], which incorporates the usage of water level sensors along with Arduino technology to make gate switching fully automated. Dam gate monitoring has been done by Kumar et al. [17] used a water level monitor and float sensor to detect the status of the dam gate. Feedback control via monitoring and data acquisition technology was achieved to implement the forward and backward operation of the gate DC motor by the programmable logic controller, which realized remote monitoring of the dam gate and the automatic control of the gate. Sun et al. [18] proposed an automated flood control scheduling model based on hormone regulation and particle swarm optimization. Zhu et al. [19] applied the multi-objective optimization control model, 1D hydrodynamic model, and multi-objective genetic algorithm to optimize the water diversion project with a series of gates during the flow regulation period, not only optimizing the adjustment frequency but also strengthening the control effect. Zhou et al. [20] used IoT technologies to establish an automatic control system for the Yangzhuang Sluice Gate to automatically monitor and manage the power distribution system and gates and improve the gate scheduling effect. Gan et al. [21] utilized reinforcement learning methods to optimize the real-time scheduling control model for a series of gates in open channel and enhance pump station operating efficiency and save energy consumption. The current studies are concentrated on the intelligent operations of single gates with few studies on joint scheduling control of water conservancy hub complexes. The multi-agent collaboration technologies refer to a series of technologies in which many agents collaborate with each other and communicate with each other to achieve their common goals [22]. As the further development of multi-agent systems, the features such as distribution, parallel, self-organization, and adaptability of them have high consistency with joint regulation management of water conservancy hub complexes [23, 24].

The proposed research on intelligent gate control of dam complexes using reinforcement learning is described in the paper. The conditions and parameters required for constructing the multi-agent reinforcement learning framework are elaborated. Then, the decomposition technique is presented to solve the flood control scheduling problem for dam complexes. Several agents are used to solve the subproblems generated after decomposing the original problem. Multiple optimal solutions will be produced in parallel from the multi-agent reinforcement learning system in response to the same flood event; thus, the multi-objective

optimization problem is solved. Lastly, the reinforcement learning algorithm is explained, demonstrated, and tested by applying a relatively simpler example project and by performing an experiment on the joint flood control and water resource scheduling of a dam complex along a straight river channel.

2 Method

2.1 Development of a Joint Control Model for Dam Groups

The isomorphous multi-agent reinforcement learning algorithm is used in this experiment. Isomorphous multi-agent reinforcement learning is the type of reinforcement learning where several agents possess similar characteristics and functions. The use of this algorithm allows for simultaneous learning and making decisions by the agents, where each agent can focus on different issues.

2.1.1 Construction of Isomorphic Multi-Agent Coupling Models

Agent: The number of homogeneous multi-agents used for this operating condition is the same as the number of control gates. All the agents have the capability of selecting their actions independently by using a discrete action distribution. Their actions range within [0%,100%] gate openings [25]. The agents perform actions independently by sampling randomly the action values that belong to their probability distributions at each time step.

Environment Module: Following the completion of hydraulic modeling on EPANET, the generated action sets through reinforcement learning are exported to the control files of each TCV gate setting in the model through Python script. After that, the states of the system are gathered.

Reward Function: The reward function for this scenario is mainly focused on the target flow and spillway discharge. In this operating condition, satisfying the entire system constraints at each time step becomes a primary consideration. Upon successfully meeting the requirements set by the conveyance system, such as obtaining the target flow rate and allowable spillway discharge, the agent is rewarded. Otherwise, it is penalized.

2.1.2 Constraints

(1) Maximum Flow Rate

As mentioned previously, the gates and dams for the water conservancy hub are associated with several river passages. In this paper, according to the design flow rate of each river passage determined by the actual construction project, the maximum flow rate of each passage is 6300L/S.

(2) Water Demand at Diversion Points

Water demand at diversion points is important when considering the stable operation of water conservancy hub gates and dams. It enables dispatchers to effectively adjust the current flow rate of rivers and allocate sufficient water supply according to the actual situation of each region or node, thus avoiding shortage or surplus. As a result, to better satisfy various water demands, achieve more effective adjustment and water allocation in the dam complex system, and maintain its stable performance, the minimum and maximum flow rates q_j of each diversion point are set based on the actual construction project.

(3) Overflow Volume

Overflow occurs when there is excess or shortage of water supply because of poor control of gates, causing water waste. In order to decrease the overflow volume and achieve effective water transmission, the overflow flow rate of this project should be controlled as follows:

$$\hat{Q}_i = 0 (i = 1, 2, 3) \quad (1)$$

In the equation, \hat{Q}_i represents the overflow discharge of each overflow channel.

2.2 Multi-Decision Solution Methods for Flood Control Dispatch

2.2.1 Decomposition-Based Multi-Objective Problem Solving Methods

The proposed reinforcement learning structure presented in this paper has an action space of dimension 500 and state space of dimension 11. This might decrease efficiency during learning as it encounters these dimensions. Flood control scheduling involves many changes in objective priorities. Penalty methods and Chebyshev methods are less flexible compared to the weighted sum method when adjusting objective priorities. In reinforcement learning, agents learn the best policy through the process of interacting with the environment. For multi-objective problems, penalty methods and Chebyshev methods need other techniques to be applied. Thus, it might not be easy to integrate them into the reinforcement learning structure. Therefore, in this paper, we use the weighted sum method for decomposition for the flood control scheduling problem for a group of dams.

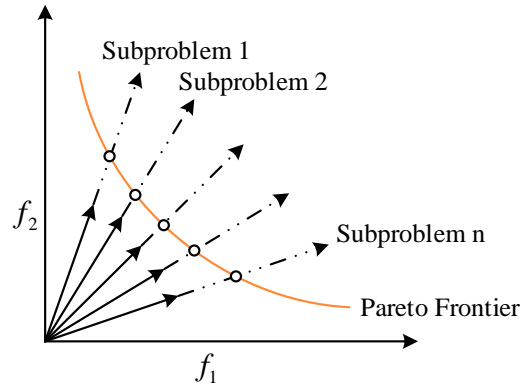


Figure 1: Schematic diagram of decomposition of multi-objective optimization problem

Break down the main problem into some sub-problems. It is possible to move along the Pareto frontier to get optimal solutions of different sub-problems through the manipulation of the weight vector in the Weighted Sum Method. Different sub-problems can be defined as the following:

$$g^{ws}(x | w) = \sum_{i=1}^k w_i f_i(x) \quad (2)$$

In the equation above, w represents the weight vector. The technique of weight summation works excellently for problems that have objective functions and rules of Pareto front relatively easy. Its implementation is straightforward and intuitive, enabling systematic exploration of the entire Pareto frontier through weight adjustments. By decomposing the multi-objective flood control scheduling problem for a group of dams into n sub-problems using the

weighted sum method, and then solving each subproblem with deep reinforcement learning algorithms, the complete Pareto frontier for the multi-objective flood control scheduling of the dam group can be obtained.

2.2.2 Solving Multi-Decision Problems for Dam Groups Based on Multi-Agent Reinforcement Learning

A multi-agent reinforcement learning approach is employed, wherein each agent shares the same model architecture but is trained using distinct reward functions. The core principle of this method involves decomposing a multi-objective problem into multiple subproblems, each focused on optimizing a specific objective and handled by an independently trained agent. Thus, although all agents share identical model structures, their differing reward functions enable them to specialize in learning how to perform optimally on their assigned objectives [26].

This paper employs a weighted summation approach to address flood control scheduling for dam clusters. When applying a multi-agent reinforcement learning framework to solve multi-objective optimization problems, effective trade-offs between objectives can be achieved by designing distinct reward criteria for each agent and integrating weighted summation principles. Specifically, each agent is trained according to its specific reward criteria, while weights are utilized to synthesize these diverse reward metrics. Let vector $r = (r_1, r_2, \dots, r_n)$ represent the set of reward values obtained by n agents for their respective optimization objectives. The weight vector $w = (w_1, w_2, \dots, w_n)$ denotes the set of optimization objective weights for the subproblems corresponding to different agents. Here, $w_i = (w_i^1, \dots, w_i^k)^T$ and $r_i = (r_i^1, \dots, r_i^k)^T$, where k denotes the number of optimization objectives. Based on the above analysis, the dam group scheduling problem is decomposed into n subproblems, with each subproblem corresponding to an agent. The optimization objective for the i th subproblem corresponding to an agent is given by Equation (3):

$$\max g^{ws}(x | w_i^j) = \sum_{i=1}^k w_i^j r_i^j \quad (3)$$

Agents solve subproblems by converting their optimization objectives into rewards and maximizing the sum of rewards corresponding to multiple objectives. Based on weighted sum decomposition, reinforcement learning models can flexibly adapt to diverse task requirements, effectively balancing potential conflicts among multiple objectives. This enables them to find solutions in multi-objective optimization contexts that satisfy individual goals while optimizing overall performance as much as possible. By applying this kind of decomposing method, every individual agent can solve their own sub-problem independently while reducing the difficulty of a single model trying to incorporate all the objectives at once. This method makes use of the power of the reinforcement learning technique to adjust itself based on the environment while maximizing rewards. However, unlike the traditional approach, this method is able to make good decomposition and parallel computation of a complex multi-objective problem through distribution of various objectives to several agents. In addition, this decomposition method utilizes diversity, whereby different agents will find different ways of optimizing their objectives, thus making contributions of diverse solutions and approaches to solving the problem in question. Through utilization of multiple agents based on the same model but with different objectives, this method efficiently solves complex multi-objective problems.

Based on the decomposed several flood control scheduling sub-problems, an agent is designed for each sub-problem, and a multi-decision system is obtained by training a number

of agents that meet different sub-problem tasks and then combining them together to obtain a multi-decision system, through this system, after inputting a flood data, different preferred solutions can be obtained, and the purpose of multi-decision is achieved, and the multi-agent solves the flood control scheduling problem of the dam group as shown in Fig. 2, the original flood control and scheduling problem of the dam group will be decomposed into n sub-problems, and a n set of reward criteria is designed. These reward criteria are combined with the inlet and outlet models of the dam group to obtain n reinforcement learning environment, and the existing flood data is used to train on these n reinforcement learning environments to obtain n reinforcement learning agents, and the weights of these n agents are extracted to form a set of weights. Finally, a number of decision-making schemes are obtained that constitute the decision solutions of all sub-problems.

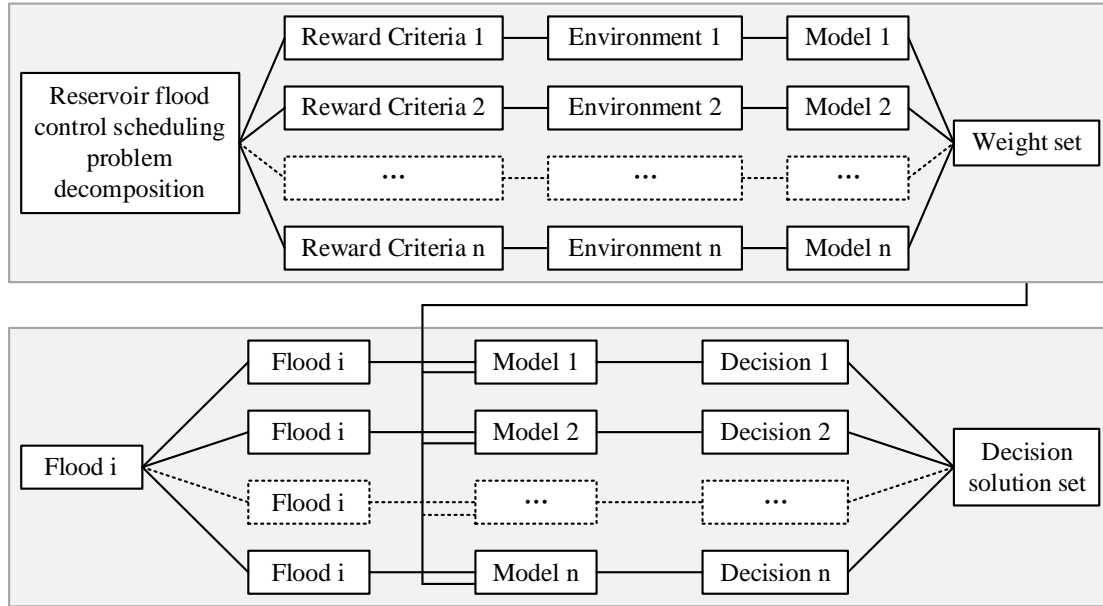


Figure 2: Schematic diagram of multi-agent solution

The formal description of the specific solution scheme is as follows: During the training phase, let the reward criterion be principle. For subproblem i , the target maximum reservoir water level is h_i , and the reward rule derived from its criterion is R^i . Then:

$$R^i = \text{principle}(h_i) \quad (4)$$

The target water level set $H = \{h_1, \dots, h_n\}$ corresponding to the n subproblems yields the reward rule set R :

$$R = \text{principle}(H) = [R^1, \dots, R^n] \quad (5)$$

Construct an initial model m_i for each subproblem, then the set of all subproblem models is:

$$M = (m_0, \dots, m_n) \quad (6)$$

The formalization of model training based on the reward set R is as follows, where E denotes the set of all subproblem reinforcement learning environments. The model is trained through the designed rewards and reinforcement learning environments:

$$M' = M \leftarrow (R \times E) = [m'_1, \dots, m'_n] \quad (7)$$

During the inference stage, when reasoning about flood W , a set of solutions for different subproblems is obtained based on the trained model ensemble, as shown below:

$$X = M' \times W = [x_0, \dots, x_n] \quad (8)$$

$$x_i = [x_i^0, \dots, x_i'] \quad (9)$$

X represents the optimal solution set for flood W . Mapping this set onto the objective space yields the Pareto frontier of our method.

Below we introduce the specific design pattern for the reward criterion. With a target maximum reservoir water level of 336 meters, two parameters are designed: $Z_{upper} = 26$ and $Z_{lower} = 24$. Rewards are assigned to the agent based on these constraints. Based on this design approach, assuming the target maximum reservoir water level for the subproblem is h_i , we set Z_{upper} and Z_{lower} to values greater than and less than the target by 0.5 meters, respectively, namely:

$$Z_{upper} = h_i + 0.5 \quad (10)$$

$$Z_{lower} = h_i - 0.5 \quad (11)$$

And incorporate the weight vector into the final reward calculation, namely:

$$r = r_{z_upper} \cdot w_1^j + r_{z_upper} w_1^j + r_{o_upper} w_2^j \quad (12)$$

Here, w_1^j represents the weight of the first optimization objective for the j th subproblem, while w_2^j represents the weight of the second optimization objective for the j th subproblem.

3 Results and Discussion

3.1 Discussion of Project Results

3.1.1 Case Study of a Channel Section

This section of the project case primarily considers the coordinated operation between the diversion gate and the control gates. The main canal section spans 15 km, while the diversion outlet section measures 5.3 km. The canal cross-section is trapezoidal with a base width of 10 m, a slope gradient of 1/25,000, and a roughness coefficient of 0.015. The upper boundary condition is a fixed water level boundary. with both the downstream channel boundary and the diversion outlet boundary governed by water level-discharge relationship curves. The project incorporates three gates: two control gates and one diversion gate. Through the coordinated

operation of Control Gate 1 and the diversion gate, the water level upstream of Control Gate 1 is maintained at the target level while satisfying the water demands of the diversion outlet and downstream areas.

In regard to the reinforcement learning algorithm of this particular case study, the major parameters are set as follows:

Agent: In our case, the agent corresponds to the control process of the dam cluster consisting of the Control Gate 1 and diversion gate. In multi-gate scenarios, the agent must consider the action distributions across multiple gates and the optimization approach for the Actor network. Similar to multi-control-gate joint regulation, separate neural networks must be constructed for Control Gate 1 and the Diversion Gate. During updates and optimization, importance sampling is applied to the action distributions of both groups. The sampled results are multiplied and their logarithms are used in the Actor network optimization process.

State Vector: Unlike multi-channel section dam group joint scheduling, this scenario involves a diversion channel section where water level and flow rate also warrant attention. It necessitates ensuring the steady-state water level upstream of Control Gate 1, the steady-state water level upstream of the Diversion Gate, the flow rate downstream of Control Gate 1, and the flow rate downstream of the Diversion Gate. Therefore, the water level upstream of Control Gate 1, the flow downstream of Control Gate 1, the water level upstream of the Diversion Gate, and the flow downstream of the Diversion Gate are selected as the state vector.

Environmental Module: After modeling the example channel section in HEC-RAS software, Python is used to write the randomly generated action sets from reinforcement learning into the opening control files for Control Gate 1 and the Diversion Gate. The resulting state vectors are then extracted.

Reward Function: The reward function is primarily designed around target water levels and target flow rates. Under this operating condition, the water level upstream of Control Gate 1, the flow rate downstream of the gate, the water level upstream of the diversion gate, and the flow rate downstream of the gate must be considered. Function types and weight settings are configured for these four hydraulic parameters.

3.1.2 Discussion of Engineering Results

For the example project of a multi-channel section gate-dam complex, we continue to discuss the design of the reward function. This function involves four target parameters: the upstream water level at Gate 1, the downstream flow rate at Gate 1, the upstream water level at the diversion gate, and the downstream flow rate at the diversion gate. The following table designates them as G1, G2, G3, and G4 respectively. The reward function is designed by considering different function types and target parameter weights, with specific function details shown in Table 1.

Table 1: The statistical table about reward functions

| Grade | Function type | Weight information |
|-------|--------------------|---------------------|
| 1 | Linear function | G1:G2:G3:G4=1:1:1:1 |
| 2 | Linear function | G1:G2:G3:G4=1:1:1:5 |
| 3 | Linear function | G1:G2:G3:G4=1:1:5:1 |
| 4 | Quadratic function | G1:G2:G3:G4=1:1:1:1 |
| 5 | Quadratic function | G1:G2:G3:G4=1:1:1:5 |
| 6 | Quadratic function | G1:G2:G3:G4=1:1:5:1 |
| 7 | Quadratic function | G1:G2:G3:G4=1:5:5:1 |
| 8 | Quadratic function | G1:G2:G3:G4=5:1:5:1 |
| 9 | Quadratic function | G1:G2:G3:G4=1:5:5:1 |

To distinguish between control gate and diversion gate water level and flow data, the upstream water level of Control Gate 1 is designated as Target Water Level 1, with the downstream flow as Target Flow 1. The upstream water level of the diversion gate is designated as Target Water Level 2, with the downstream flow as Target Flow 2. Across the nine experiments, all parameters remained identical except for the reward function type. The four target parameters were: Target Water Level 1: 61.89 m, Target Water Level 2: 61.93 m, Target Flow Rate 1: 122 m³/s, Target Flow Rate 2: 132 m³/s. Analyzing the reinforcement learning process under the nine reward functions, we first examine their respective reward convergence patterns. The reward trend plots for different functions are shown in Figure 3. The trend of reward convergence was observed throughout the nine experiments. However, this convergence trend appears not so strong in experiments 1, 2, and 8. For instance, the convergence trend in Experiment 1 is very weak. In Experiment 2, the reward remained stable during the first half of iterations but exhibited significant fluctuations in the latter half. Experiment 8 showed no noticeable changes in reward throughout the entire iteration process, maintaining overall stability. Therefore, based on the reward convergence plots, these three experiments failed to optimize the four target parameters through gate opening adjustments.

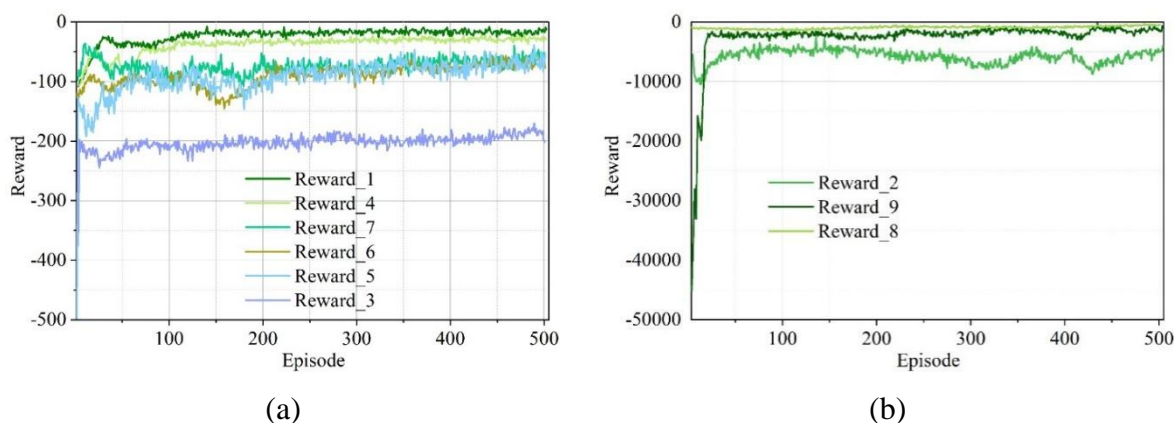


Figure 3: The tendency chart of reward about different reward functions

Statistical analysis of water level data reveals the changes in water levels 1 and 2 under different reward functions, as shown in Tables 2 and 3 respectively. It can be observed that although significant fluctuations occurred in water level 2 during the later stages of Experiment 2, the majority of these fluctuations remained within the target range. For target water level 1, Experiment 2 achieved a 75.65% probability of maintaining fluctuations within ± 0.1 m of the target level after convergence. For target water level 2, Experiment 2 can ensure with 88.6% probability that the water level fluctuates within ± 0.1 m of the target level. Regarding water level data, the remaining eight experiments all ensure with over 99.63% probability that water level data remains within the ± 0.1 m compliance range during the later stages of iteration.

Table 2: The results of nol water level of different reward functions

| Indicator | Serial Number 1 | Serial Number 2 | Serial Number 3 | Serial Number 4 | Serial Number 5 | Serial Number 6 | Serial Number 7 | Serial Number 8 | Serial Number 9 |
|---|-----------------|-----------------|-----------------|-----------------|-----------------|-----------------|-----------------|-----------------|-----------------|
| Target water level /m | 61.89 | 61.89 | 61.89 | 61.89 | 61.89 | 61.89 | 61.89 | 61.89 | 61.89 |
| Average water level /m | 61.87 | 61.26 | 61.45 | 61.42 | 61.45 | 61.16 | 61.22 | 61.25 | 61.25 |
| Maximum water level /m | 61.92 | 61.3 | 61.82 | 61.83 | 61.62 | 61.2 | 61.34 | 61.32 | 61.47 |
| Minimum water level /m | 61.81 | 61.22 | 61.07 | 61 | 61.27 | 61.12 | 61.1 | 61.18 | 61.02 |
| Water level range /m | 0.11 | 0.08 | 0.75 | 0.83 | 0.35 | 0.08 | 0.24 | 0.14 | 0.45 |
| MAE | 0.02 | 0.06 | 0.01 | 0.02 | 0.02 | 0.03 | 0.01 | 0.14 | 0.02 |
| RMSE | 0.02 | 0.08 | 0.06 | 0.04 | 0.02 | 0.03 | 0.02 | 3.09 | 0.05 |
| Water level compliance rate /% ($\pm 0.2m$) | 100 | 99.42 | 100 | 100 | 100 | 100 | 100 | 100 | 100 |
| Water level compliance rate /% ($\pm 0.1m$) | 100 | 75.65 | 100 | 100 | 100 | 100 | 100 | 99.63 | 100 |

Table 3: The results of no2 water level of different reward functions

| Indicator | Serial Number 1 | Serial Number 2 | Serial Number 3 | Serial Number 4 | Serial Number 5 | Serial Number 6 | Serial Number 7 | Serial Number 8 | Serial Number 9 |
|---|-----------------|-----------------|-----------------|-----------------|-----------------|-----------------|-----------------|-----------------|-----------------|
| Target water level /m | 61.93 | 61.93 | 61.93 | 61.93 | 61.93 | 61.93 | 61.93 | 61.93 | 61.93 |
| Average water level /m | 61.89 | 61.28 | 61.47 | 61.69 | 61.46 | 61.19 | 61.23 | 61.26 | 61.26 |
| Maximum water level /m | 61.93 | 61.33 | 61.86 | 61.87 | 61.64 | 61.22 | 61.35 | 61.33 | 61.49 |
| Minimum water level /m | 61.85 | 61.23 | 61.08 | 61.5 | 61.28 | 61.15 | 61.11 | 61.19 | 61.03 |
| Water level range /m | 0.08 | 0.1 | 0.78 | 0.37 | 0.36 | 0.07 | 0.24 | 0.14 | 0.46 |
| MAE | 0.05 | 0.04 | 0.04 | 0.05 | 0.03 | 0.06 | 0.02 | 0.17 | 0.05 |
| RMSE | 0.05 | 0.05 | 0.03 | 0.02 | 0.02 | 0.03 | 0.02 | 3.09 | 0.05 |
| Water level compliance rate /% ($\pm 0.2m$) | 100 | 100 | 100 | 100 | 100 | 100 | 100 | 100 | 100 |
| Water level compliance rate /% ($\pm 0.1m$) | 100 | 88.6 | 100 | 100 | 100 | 100 | 100 | 99.63 | 100 |

Statistical analysis of flow data from nine experimental groups is presented. The results for flow 1 and flow 2 under different reward functions are shown in Tables 4 and 5, respectively. Comparing the water level data distributions reveals significant differences in flow data distribution, with flow compliance rates lower than water level compliance rates. For target flow 1, experiments 4, 5, and 9 demonstrate superior control capabilities. For target flow rate 2, experiments 2, 4, 5, 7, and 9 demonstrated superior control capabilities. Considering the weighting of the four target parameters in the reward functions across the nine experiments, the

weight assigned to flow rate 2 in the reward functions of experiments 2, 5, 7, and 9 was significantly greater than that for flow rate 1. Consequently, the compliance rates for flow rate 2 were markedly better than those for flow rate 1 in these four experiments. The quadratic reward functions represented by experiments 4, 5, 7, and 9 demonstrated superior flow control compared to linear reward functions. Experiments 4 and 5, which emphasized flow weighting, achieved markedly better control of both target flows than the other experimental groups.

Table 4: The results of no1 quantity of flow of different reward functions

| Indicator | Serial Number 1 | Serial Number 2 | Serial Number 3 | Serial Number 4 | Serial Number 5 | Serial Number 6 | Serial Number 7 | Serial Number 8 | Serial Number 9 |
|---|-----------------|-----------------|-----------------|-----------------|-----------------|-----------------|-----------------|-----------------|-----------------|
| Target flow rate /m ³ /s | 122 | 122 | 122 | 122 | 122 | 122 | 122 | 122 | 122 |
| Average flow rate/m ³ /s | 130.23 | 79.47 | 132.78 | 116.67 | 115.81 | 131.87 | 107.64 | 134.35 | 119.85 |
| Maximum flow rate/m ³ /s | 134.61 | 117.49 | 133.53 | 124.89 | 122.05 | 134.8 | 114.88 | 140.09 | 128.58 |
| Minimum flow rate/m ³ /s | 125.84 | 41.45 | 132.03 | 108.45 | 109.56 | 128.94 | 100.39 | 128.61 | 111.12 |
| Extremely poor traffic/m ³ /s | 8.77 | 76.04 | 1.5 | 16.44 | 12.49 | 5.86 | 14.49 | 11.48 | 17.46 |
| MAE | 12.58 | 26.13 | 14.35 | 2.77 | 2.63 | 14.03 | 8.57 | 13.74 | 4.51 |
| RMSE | 12.65 | 29.99 | 14.41 | 3.13 | 3.45 | 14.07 | 9.13 | 14.7 | 5.1 |
| Traffic compliance rate/(±5m ³ /s) | 0 | 4.69 | 0 | 93.66 | 81.54 | 0 | 13.54 | 0 | 59.66 |

Table 5: The results of no2 quantity of flow of different reward functions

| Indicator | Serial Number 1 | Serial Number 2 | Serial Number 3 | Serial Number 4 | Serial Number 5 | Serial Number 6 | Serial Number 7 | Serial Number 8 | Serial Number 9 |
|---|-----------------|-----------------|-----------------|-----------------|-----------------|-----------------|-----------------|-----------------|-----------------|
| Target flow rate /m ³ /s | 132 | 132 | 132 | 132 | 132 | 132 | 132 | 132 | 132 |
| Average flow rate/m ³ /s | 116.20 | 125.45 | 117.99 | 129.96 | 126.64 | 116.81 | 128.38 | 109.58 | 127.30 |
| Maximum flow rate/m ³ /s | 124.14 | 131.77 | 121.79 | 131.27 | 131.07 | 121.38 | 130.88 | 120.92 | 132.15 |
| Minimum flow rate/m ³ /s | 108.26 | 119.13 | 114.18 | 128.65 | 122.21 | 112.24 | 125.88 | 98.23 | 122.44 |
| Extremely poor traffic/m ³ /s | 15.88 | 12.64 | 7.61 | 2.62 | 8.86 | 9.14 | 5 | 22.69 | 9.71 |
| MAE | 12.72 | 2.69 | 12.72 | 0.61 | 2.65 | 12.7 | 0.86 | 20.89 | 2.19 |
| RMSE | 12.82 | 3.48 | 12.74 | 0.63 | 2.95 | 12.75 | 1.03 | 22.49 | 2.6 |
| Traffic compliance rate/(±5m ³ /s) | 0 | 85.62 | 0 | 100 | 95.63 | 0 | 100 | 0 | 96.51 |

3.2 Joint Flood Resource Dispatch Experiment

3.2.1 Basic Information on the Watershed

Tu Hai River is one of the significant rivers in the Southern Hai River Basin. It performs roles

such as regulating floods, draining, and irrigating. This river is found south of the Yellow River and the Jin Di River embankment. This river connects with the Ma Jia River and Dehui New River basins in the north direction. It starts from Nanle County in Henan Province and discharges in the Bohai Sea in Zhanhua County of Shandong Province. The length of the river is 436.35 km, and its basin area is 13,918.7 km². In Shandong Province, it has a river length of 406 km and basin area of 13,312.7 km². In the Tu-Hai River basin, there are eleven tributaries whose basin area is greater than 300 km²: Zhaoni New River, Old Zhaoni River, Tumasha River, Qinkou River, New Jinxian River, Zhaowang River, Shangsi New River, West New River, Qili River, Wei River, and Sha River.

The mainstream of Tu-Hai River has a total of 19 sluice dams within Shandong Province. The drainage basin of Tu-Hai River holds a high density population and acts as a critical area for irrigation of agriculture in northern Shandong by diverting water from the Yellow River. Water resources have become exceedingly scarce in the area. Over-extraction of groundwater has reached close to the maximum total groundwater use indicator. Competition for agricultural and ecological water between urban domestic and industrial activities is especially notable in the area.

3.2.2 Flood Selection

(1) Selection of Representative Flood Events. Statistical analysis of annual peak flood events at Baoji Weir from 1971 to 2012 identified representative flood years: the above-average flood year of July 1973 (Flood No. 1), the normal-flow year of July 1984 (Flood No. 2), and the below-average flood year of July 1985 (Flood No. 3).

(2) Interval Floods. For dam-gate complex operations, upstream dam-gate scheduling influences downstream mainstem floods but typically exerts minimal impact on interval floods. Therefore, interval floods from major tributaries serve as flood inputs. Based on the distribution of major tributaries, nine tributary source-discharge nodes were established for this flood source-discharge node configuration. From upstream to downstream, these are: Starting Point, Xinjinxian River, Zhaowang River, Xixin River, Qili River, Zhaoniuxin River, Laozhaoniuxin River, Dasi River, and Sha River.

3.2.3 Example Calculations

(1) Constraint Parameters

(a) Cascade Weirs and Dams. Fourteen water gates and five rubber dams along the route participate in coordinated operation. Considering the effects of storage water level and flood control water level, the storage water level during floods does not exceed the flood control water level, with an effective total reservoir capacity of 100.1 million m³.

(b) Ecological Flow. Statistical analysis of measured flows at Wangdikou, Liuqiao, Gongjia, and Baoji weirs from 1970 to 2013 shows multi-year average flood season flows of 6.5, 16.5, 27.1, and 48.9 m³/s, respectively. Based on known control areas and average flows for existing gates and dams, average flows for other structures were estimated using linear interpolation according to their control areas. River ecological flows were calculated using the Tennant method. During floods, ecological flows at cross-sections were controlled at 30%–40% of the multi-year average flood flow, with gate/dam control flows ranging from 0.6 to 16 m³/s. Detailed water level and flow control parameters are shown in Table 6.

(c) Timing of Water Storage. During the first stage of flood control, open spillway control is maintained until the flood peak. Water storage begins during the drawdown phase of the second stage, when flood discharge falls below drainage flow. The discharge from gates and dams shall not be less than the downstream ecological control flow.

(d) River Cross-Sections. The Tuhai River uses calculated cross-section data with about 500

meters intervals. The roughness coefficient of the main channel is 0.028 and that of the floodplain is 0.05. The terminal elevation of the river is regulated by the level of tidal water at the estuary.

Table 6: Adjust result and control parameters of water level and ecological flow

| Gate dam | Control parameter | | | | | The results of the water level adjustment at the end of the day | | |
|-----------------------|----------------------|----------------------------------|------------------------------------|--|---|---|---------|---------|
| | Design water level/m | Design waterlogged water level/m | Control water level/m on the brake | Average traffic flow in flood season/ ($m^3 \cdot s^{-1}$) | Ecological control flow/ ($m^3 \cdot s^{-1}$) | Flood 1 | Flood 2 | Flood 3 |
| Remote temple brake | 44.12 | 44.66 | 43.45 | 1.35 | 0.81 | 42.3 | 42.63 | 41.44 |
| Horse lock | 43.03 | 43.37 | 43.8 | 1.8 | 0.84 | 41.32 | 42.86 | 40.69 |
| China gate | 37.38 | 36.05 | 35.78 | 3.1 | 1.27 | 35.87 | 38.12 | 38.35 |
| Young gate | 36.75 | 38.71 | 35.72 | 3.18 | 0.82 | 34.34 | 35.25 | 35.69 |
| Zhenzhuang rubber dam | 37.62 | 35.36 | 34.4 | 4.6 | 1.81 | 33.82 | 33.39 | 35.89 |
| King's wall brake | 34.21 | 30.99 | 33.94 | 6.55 | 2.38 | 32.22 | 33.75 | 33.9 |
| Changdong rubber dam | 29.71 | 28.46 | 30.23 | 9.73 | 4.09 | 31.22 | 31.44 | 31.12 |
| North city rubber dam | 30.58 | 29.26 | 30.94 | 10.81 | 4.03 | 27.55 | 28.95 | 28.58 |
| Booping gate | 28.52 | 29.31 | 27.98 | 13.22 | 5.25 | 28.04 | 28.92 | 29.06 |
| Pottery bridge | 27.4 | 26.44 | 29.31 | 13.61 | 5.4 | 26.29 | 27.81 | 27.41 |
| Bridge lock | 25.09 | 25.62 | 24.58 | 16.09 | 6.03 | 24.16 | 24.52 | 24.71 |
| South gate | 20.14 | 24.08 | 19.26 | 25.19 | 7.57 | 20.51 | 20.28 | 20.57 |
| Bridge rubber dam | 21.06 | 19.62 | 20.23 | 25.65 | 7.6 | 18.89 | 19.61 | 19.26 |
| Palace brake | 18.74 | 18.68 | 16.88 | 26.68 | 8.36 | 16.79 | 17.33 | 16.61 |
| Camp brake | 14.37 | 15.97 | 14.89 | 37.94 | 11.45 | 13.96 | 14.61 | 13.49 |
| Fan bridge brake | 8.09 | 11.5 | 11.9 | 42.46 | 12.68 | 10.02 | 10.96 | 10.43 |
| hillock | 3.36 | 4.93 | 5.57 | 49.06 | 15.08 | 5.68 | 5.43 | 5.83 |
| Dam lock | 3.72 | 3.84 | 4.61 | 50.13 | 15.23 | 3.39 | 3.46 | 3.23 |
| Paraffin dam | 3.32 | 4.29 | 2.68 | 49.82 | 15.34 | 3.02 | 2.24 | 2.98 |

(2) Calculation Results

(a) Analysis of Storage Process

In the flood drawdown stage, water gates and rubber dams retained water but allowed the release of ecological base flows to maintain downstream water levels. At the end of the flood, there were some structures whose capacity was still not filled up to full. This was due to the fact that: 1. The intrinsic discharge of the flood was not enough for storing purposes; 2. On

achieving the storage level, the ecological base flows were released from the upstream structures while inflow became small and hence, resulting in a reduction in the water levels of the upstream structures. The percentages of reservoir capacity utilized during average floods in low-flow years, normal-flow years, and high-flow years were 82.1%, 95.9%, and 96.3%, respectively. If the inflow into the mainstem was for a normal-flow or high-flow flood event, then the percentage utilization of reservoir capacity would be near 95%. In the flood rise stage, the flow regime of Changdong Rubber Dam and Gongjia Weir was almost similar to natural flow regimes. However, during the flood drawdown phase, flow processes at both sites exhibited reduced magnitudes, primarily due to flood regulation implemented by the dams at this level and upstream structures during the drawdown phase. Around the third day of the flood, the minimum discharge at the Changdong Rubber Dam was the ecological control flow of 4.09 m³/s. Around the fifth to seventh day, the minimum discharge at the Gongjia Weir was the ecological control flow of 8.36 m³/s. At all other times, the discharge exceeded the ecological control flow.

(b) Water Volume Analysis.

Model calculations yielded typical flood regulation results as shown in Table 7. During the normal-flow Year 2 flood, the total flood volume was 157.2 million m³, with reservoir regulation accounting for 80 million m³ and a flood resource utilization rate of 50.2%. During the simulation periods of the three typical floods, the flood resource utilization rate did not exceed 60%. The highest utilization rate was 58.5% for Flood No. 1 in the low-water year, while the lowest was 35.5% for Flood No. 3 in the high-water year. This indicates that as flood magnitude increases, the flood utilization rate shows a decreasing trend.

Table 7: Typical flood adjust result

| Flood | Initial Water Volume/ Hundred Million M ³ | Input Volume/ Hundred Million M ³ | Output Water Volume/ Hundred Million M ³ | Total Water Storage Capacity/ Hundred Million M ³ | Flood Storage Capacity/ Hundred Million M ³ | Utilization Rate of Flood Resources/% | Storage Capacity Utilization Rate/% |
|---------|---|---|--|---|---|---------------------------------------|-------------------------------------|
| Flood 1 | 0.312 | 1.266 | 0.537 | 1.062 | 0.759 | 58.5 | 82.1 |
| Flood 2 | 0.312 | 1.572 | 0.766 | 1.127 | 0.8 | 50.2 | 95.9 |
| Flood 3 | 0.312 | 2.336 | 1.492 | 1.161 | 0.838 | 35.5 | 96.3 |

(c) Comparison of simulated and measured storage volumes. Through coordinated regulation, the three sluice gates—Liuqiao, Gongjia, and Baoji—increased their total regulated storage volumes by 7.19 million m³, 9.88 million m³, and 11.36 million m³ respectively during Floods 1, 2, and 3. As flood magnitude increased, regulated storage volumes correspondingly expanded. During normal-runoff and high-runoff years, the simulated storage capacities at main-channel gates and dams were largely consistent, indicating that the gate-dam complex could achieve near-full storage levels in normal-runoff years. For flood events in normal-flow years, the simulated storage capacity in this simulation was approximately double the actual storage volume. The above-mentioned operation ensured efficient utilization of the floodwater through proper coordination between gate and dam operations that would enable the storing of water immediately while losing minimal amounts of water.

(3) Risk Identification

There are two hazards involved in the process of utilizing the floodwater from the sluices and the dams. The first one is the risk of creating an artificial flood. When all gates are closed or partially opened for storage, two risks arise: First, when significant upstream inflow occurs, gates must be opened for discharge, potentially causing artificial floods downstream. Second, with high water levels upstream of the gates, delayed discharge during heavy upstream floods

may lead to floodplain overflow, causing inundation damage. The second is the risk of insufficient water storage. If gates are closed too late and flood inflows are small, the stored water volume may fail to meet design requirements, resulting in inadequate utilization of flood resources. Joint reservoir storage by gates and dams is closely influenced by flood processes in both main and tributary rivers. Modern meteorological forecasting technologies should be integrated to predict flood development trends in both main and tributary rivers in advance, enabling coordinated flood control and benefit-oriented scheduling for gate and dam clusters.

4 Conclusion

Under constraints such as flood control and ecological flow requirements, draft scheduling rules for water gates and rubber dams. Consider the impact of flood sources and sinks within the section, and employ multi-agent technology to achieve coordinated water storage scheduling for dam clusters, thereby enhancing overall benefits. Based on a case study, this research investigates the configuration of reward functions and fundamental parameters in reinforcement learning models. Results indicate that reward function types significantly influence reinforcement learning models. Reinforcement learning shows high efficiency when applied in situations where the action distribution is according to a beta distribution. In other words, hyperparameters like the learning rate have little influence on the system. Dam storing capacity tends to increase while flood utilization efficiency decreases with increasing flood magnitude.

About the Author

Nan Zhu was born in Yancheng, Jiangsu, China, in 2002. He obtained a bachelor's degree from Beijing Institute of Technology in China. He is currently studying at the College of Engineering, City University of Hong Kong. His main research direction is the interdisciplinary application of advanced mechanical engineering.

References

- [1] Xu, A., Yang, L. E., Yang, W., & Chen, H. (2020). Water conservancy projects enhanced local resilience to floods and droughts over the past 300 years at the Erhai Lake basin, Southwest China. *Environmental Research Letters*, 15(12), 125009.
- [2] Wu, Y., Guo, L., Xia, Z., Jing, P., & Chunyu, X. (2019). Reviewing the Poyang lake hydraulic project based on humans' changing cognition of water conservancy projects. *Sustainability*, 11(9), 2605.
- [3] Xingwen, L. (2021). Research on water conservancy project construction and operation management based on cost management. In *E3S Web of Conferences* (Vol. 276, p. 01034). EDP Sciences.
- [4] Erpicum, S., Crookston, B. M., Bombardelli, F., Bung, D. B., Felder, S., Mulligan, S., ... & Palermo, M. (2021). Hydraulic structures engineering: An evolving science in a changing world. *Wiley Interdisciplinary Reviews: Water*, 8(2), e1505.
- [5] Niu, X. (2022). The Three Gorges Project. *Engineering*, 15(8), 17-23.

- [6] Liu, Q., Fang, G. H., Sun, H. B., & Wu, X. W. (2017). Joint optimization scheduling for water conservancy projects in complex river networks. *Water Science and Engineering*, 10(1), 43-52.
- [7] Peng, Z., Hu, W., Zhang, Y., Liu, G., Zhang, H., & Gao, R. (2021). Modelling the effects of joint operations of water transfer project and lake sluice on circulation and water quality of a large shallow lake. *Journal of Hydrology*, 593, 125881.
- [8] Hailu, M. G., & Thakur, A. (2018). Design analysis of water control gate for diversion dams. *International Journal of Current Engineering and Technology*, 8(3), 708-718.
- [9] Bocko, J., Pastor, M., Hagara, M., & Lengvarský, P. (2023). Identification of the failure causes of the water dam gate valves control mechanism. *Engineering Failure Analysis*, 152, 107468.
- [10] Lu, S. (2022, December). Research and practice on the intelligent transformation of the gate control system in a large hydropower station. In *Journal of Physics: Conference Series* (Vol. 2399, No. 1, p. 012038). IOP Publishing.
- [11] Li, S., Zhang, B., Tong, G., Li, Y., Liu, Z., Shi, B., ... & Gan, Z. (2025). Online Intelligent Monitoring System and Key Technologies for Dam Operation Safety. *Advances in Civil Engineering*, 2025(1), 9983255.
- [12] Luo, W., Wang, C., Zhang, Y., Zhao, J., Huang, Z., Wang, J., & Zhang, C. (2025). A deep reinforcement learning approach for joint scheduling of cascade reservoir system. *Journal of Hydrology*, 651, 132515.
- [13] Su, C., Wang, P., Yuan, W., Cheng, C., Zhang, T., Yan, D., & Wu, Z. (2022). An MILP based optimization model for reservoir flood control operation considering spillway gate scheduling. *Journal of Hydrology*, 613, 128483.
- [14] Mou, S., Qu, T., Li, J., Wen, X., & Liu, Y. (2024). Joint optimal use of sluices of a group of cascade hydropower stations under high-intensity peak shaving and frequency regulation. *Water*, 16(2), 275.
- [15] Yang, J., Zhang, H., Zeng, H., Wei, X., Lei, H., Chen, J., ... & Yang, Q. (2024, September). Key Technology of Multi-Objective One-Key Opening and Closing of Hydropower Station Gate. In *2024 6th International Symposium on Robotics & Intelligent Manufacturing Technology (ISRIMT)* (pp. 157-160). IEEE.
- [16] Hamidun, M. A. H., & Ibrahim, S. A. (2022). Dam Gate Automation Control System by Using Arduino. *Progress in Engineering Application and Technology*, 3(1), 683-690.
- [17] Kumar, A., Pal, V. K., Chaurasiya, V. K., & Singh, A. (2021). Dams Gate Control Using Programmable Logic Controller and SCADA. *International Journal*, 9(3), 195-198.
- [18] Sun, A., Hu, D., Shan, C., & Wang, J. (2023). Automatic scheduling and control technology of pump gate clusters of regional water conservancy project. *Desalination and Water Treatment*, 293, 82-88.
- [19] Zhu, J., Zhang, Z., Lei, X., Yue, X., Xiang, X., Wang, H., & Ye, M. (2021). Optimal

- regulation of the Cascade Gates Group Water Diversion Project in a flow adjustment period. *Water*, 13(20), 2825.
- [20] Zhou, W., Chen, S., Zou, W., Yang, J., & Wu, M. (2022, February). Intelligent decision-making system for realizing the automatic control of Yangzhuang sluice based on the internet of things technology. In *Journal of Physics: Conference Series* (Vol. 2187, No. 1, p. 012011). IOP Publishing.
- [21] Gan, T., Jiang, Y., Zhao, H., He, J., & Duan, H. (2024). Research on low-energy consumption automatic real-time regulation of cascade gates and pumps in open-canal based on reinforcement learning. *Journal of Hydroinformatics*, 26(7), 1673-1691.
- [22] Meng, M. (2024). Construction of Ecological Water Resources Management Leadership Model Based on Multi-Agent Collaboration. *Water Resources Management*, 38(15), 5809-5822.
- [23] Shen, Z., Liu, P., Ming, B., Feng, M., Zhang, X., Li, H., & Xie, A. (2018). Deriving optimal operating rules of a multi-reservoir system considering incremental multi-agent benefit allocation. *Water Resources Management*, 32(11), 3629-3645.
- [24] Yang, Y., Wang, P., Liu, X., Luo, W., & Yang, L. (2025). A Multi-Agent and GraphRAG-Based Framework for Operation and Management Decision-Making in Hydraulic Projects. *Water Resources Management*, 1-23.
- [25] Cen Wen. (2012). The Study on Water Conservancy Project Control System. *Applied Mechanics and Materials*, 1800(170-173), 1996-1999.
- [26] Xiaoyu Wang & Fengping Wu. (2024). Assessment of reclaimed water utilization in water-scarce regions of China: A multi-dimensional–multi-agent coupling and nesting perspective. *Journal of Cleaner Production*, 450, 141815-.